J. Physiol. (1981), **317**, *pp.* 347–364
With 9 text-figures
Printed in Great Britain

EFFECT OF pH ON THE FORMATION AND DECAY OF THE METARHODOPSINS OF THE FROG

BY CH. BAUMANN AND W. ZEPPENFELD

From the Physiologisches Institut, Justus Liebig-Universität, D-6300 Giessen, Federal Republic of Germany

(*Received 24 October 1980*)

SUMMARY

1. Suspensions of membrane vesicles were prepared by sonication of dark-adapted frog rod outer segments. The pH was adjusted to one of twelve values between 5·0 and 9·8; the temperature was 15 °C. Each preparation was exposed to a single yellow flash of 120 μs duration, and rapid and slow changes of absorbance were measured at 475 nm wavelength.

2. Rapid changes consist of a transient rise followed by a diphasic decay to a new level of absorbance which is lower than that before the light exposure. The level of absorbance reached at the end of the rapid changes is lower at lower pH.

3. Kinetic analysis reveals that three reactants take part in the rapid reactions, viz. metarhodopsin I and two isochromic forms of metarhodopsin II named metarhodopsin II′ and metarhodopsin II″. The kinetics of the reversible transition from metarhodopsin I to metarhodopsin II′ are not measurably influenced by the pH of the medium. However, the reversible reaction of metarhodopsin II′ with metarhodopsin II″ is dependent on pH because metarhodopsin II″ is encountered either as a protonated or as a deprotonated compound.

4. Slow reactions are due to metarhodopsin I and to metarhodopsin III. A combined quantitative analysis of both rapid and slow reactions involves a reversible reaction between metarhodopsin II′ and metarhodopsin III and a hydrolysis of metarhodopsin II′ to retinal and opsin. The scheme employed accounts for the pH dependence of all equilibria although only one of the metarhodopsins reacts directly with protons.

INTRODUCTION

The metarhodopsins are unstable intermediates which occur in the bleaching sequence of rhodopsin. According to spectroscopic and kinetic evidence, three metarhodopsins can be distinguished from one another. Metarhodopsin I (MR I) and metarhodopsin II (MR II) are involved in rapid thermal reactions, and their absorbance peaks at 482 nm and 385 nm wavelength, respectively (Matthews, Hubbard, Brown & Wald, 1963). Metarhodopsin III (MR III) has absorptive properties similar to those of MR I but it reacts more slowly (Reuter, 1976).

The significance of the metarhodopsins for visual transduction and visual adaptation

is still unclear. Studies on the kinetics of the metarhodopsins may provide a means for assessing their physiological relevance. These kinetic studies were mostly confined to either an analysis of the rapid reactions alone (i.e. on a millisecond time scale) or to an analysis of the slow reactions alone (i.e. on a minute time scale). In a recent publication the two types of analysis were combined and led to evidence of the equilibrium between MR I and MR II in the frog retina (Baumann, 1978).

In the present study rapid and slow reactions of the metarhodopsins were examined at different pH. The influence of protons upon the MR I – MR II transition has been known since the first detailed description of this reaction was published by Matthews *et al.* (1963). Recently, Chabre & Breton (1979) demonstrated a reversal of MR III to MR II at low pH. Alkalinity, on the other hand, favours the formation of MR III (Bowmaker, 1973). These findings suggest that the MR I – MR II transition is not the only pH-dependent equilibrium in the sequence of the meta intermediates. Quantitative analysis of our results has confirmed this view to the extent that the kinetics of the metarhodopsins are, in fact, best described as a system of equilibrium reactions. There is, however, but one step in which protons are directly involved, and all pH effects observed are consequences of this very rapid reaction.

In a study on pH effects the rhodopsin molecules should be readily accessible to the protons of the surrounding medium. Therefore, the experiments were carried out with suspensions of rod membranes rather than with intact rods where the plasma membrane could give rise to a difference between the intracellular pH and the experimentally modified pH of the external buffers (cf. Walker & Brown, 1977).

METHODS

Preparation and sonication of rod outer segments. Frogs (*Rana esculenta*) were dark-adapted for 12 h, and all steps of the preparation were carried out in dim red light. The animals were killed, and their eyes were removed. The eyeballs were hemisected at the equator, and the retinae were floated out of the eye cup in a buffered saline solution (see below). Eight retinae were collected in a 5 ml centrifuge tube, and a small volume of 40% sucrose solution (equal to the volume of the retinae) was added. The retinae were centrifuged at 4500 *g* for 30 min. The supernatant was discarded, and the sedimented retinae were ground with a glass rod against the walls of the tube and mixed with 1·5 ml sucrose solution. This suspension was layered under buffered saline solution and centrifuged at 24.500 *g* for 45 min. Rod outer segments, aggregated at the interface between the sucrose and the buffer (Saito, 1938), were collected with a small pipette, washed and eventually suspended in 0·7 ml of cooled and buffered saline solution. Ultrasonic irradiation was applied to this suspension for 10 s (Branson B12 sonifier, horn tip diameter 3 mm, energy output 20% of maximum). Sonication was accompanied by a temperature rise but the temperature of the suspension never exceeded 20 °C. The pH was measured after sonication with a small glass electrode dipped into the freshly made suspension of membrane vesicules. According to an electron microscopic test (negative contrast with ammonium molybdate), the mean diameter of the vesicles was about 70 nm. Spontaneous sedimentation of these particles was not observed during the experiments. The suspension was transferred into a cuvette with a capacity of 0·5 ml and a depth (optical path-length) of 5 mm. The temperature was kept constant by a thermostatically controlled cooling system. The temperature was measured inside the cuvette by means of a thermistor. All experiments were carried out at 15 °C.

Suspending medium and buffers. The ionic medium used in all steps of the dissection and isolation procedure contained NaCl (50 mM), KCl (37 mM) and one of the following buffers: NaH_2PO_4/Na_2HPO_4 in the range of pH 5 to pH 8 or $Na_4P_2O_7/HCl$ for pH higher than 8. The osmolarity of the buffers was 0·048 osmol. The content of Na^+ and K^+ in the medium was modelled on the ionic composition found by Hagins & Yoshikami (1975) in frog rod outer segments.

Spectrophotometry and bleaching. The spectrophotometer consisted of two separate systems with a common sample compartment. One system was designed for the study of rapid absorbance changes and is similar to the instrument described in Baumann (1976). Its essential part is a flash-gun supplying brief, intense flashes from a xenon-filled discharge tube. Ultraviolet radiation and the shorter visible wavelengths of the flash were absorbed by a yellow glass filter (Schott OG 530/3 mm). A single yellow flash bleached 20–30 % of the rhodopsin. The photomultiplier of this system was protected by a flash-blocking filter (Schott DEKIF special 494). The measuring wavelength was 475 nm, and the frequency response of the measuring system ranged from d.c. to 55 kHz (−3 dB). After analogue-to-digital conversion, the rapid signals were stored in a small computer.

The other system was a dual-wavelength spectrophotomer designed for the recording of very slow absorbance changes where the reduction of drift was essential. For this purpose the preparations were alternately exposed to the measuring wavelength (475 nm) and to a reference wavelength (669 nm), the latter being feebly absorbed by rhodopsin. These monochromatic beams were formed by two interference filters illuminated by a d.c.-driven iodine lamp and mounted on a filter wheel. The wheel rotated at a speed of ten revolutions per second and, at this rate, an electronic network formed a voltage proportional to $(k - \log \tau_{475})$. The quantity τ_{475} is the transmission of the preparation at 475 nm; k may be considered as constant so long as two conditions are met: (i) the absorbance of the preparation does not measurably change at 669 nm wavelength; (ii) any fluctuation in the light emission of the lamp or in the sensitivity of the system affects the two wavelengths in proportion to their intensity. Slow absorbance changes *vs.* time were monitored with a pen recorder. The frequency response of the slow system was limited to $\leqslant 0{\cdot}1$ Hz by an active low-pass filter.

In both systems photomultipliers with 51 mm diameter end-on photocathodes were used. The diameter of the cylindrical cuvette was only 10·5 mm, allowing all light scattered forward to be collected by the large windows of the multipliers. The cuvette was placed in one of two positions: for pre-flash recording and registration of slow absorbance changes the cuvette was in the optical pathway of the dual-wavelength spectrophotometer and was placed next to the window of an EMI 9658 R photomultiplier. For the flash and immediately afterwards, when the rapid changes were to be recorded, the cuvette was shifted by hand momentarily to a position in front of the flash-blocking filter for the second multiplier (EMI 9634 QR). More details about the timing in the experiments may be found in the Results section.

RESULTS

Recording of rapid and slow absorbance changes

Two spectral regions are appropriate for the study of the MR I–MR II transition: the near-ultraviolet (wavelength $\approx$ 380 nm) and the visible wavelengths around 480 nm. In the former region the formation of MR II dominates the spectral changes while in the latter the formation and the decay of MR I can be recorded. Recordings at the wavelength 475 nm are the basis of the present study because here the rapid decay of MR I to MR II can be followed without interference from other intermediates. The more complex situation at the wavelength 380 nm was analysed in a previous study (Baumann, 1976). Flash bleaching was carried out 2 or 3 h after beginning the preparation when the absorbance of the suspension had reached a stable level (cf. Fig. 2). A typical recording of rapid changes following the flash is shown in Fig. 1. The flash causes a fast initial rise followed by a much longer decay. The rise is due to the transition of rhodopsin to MR I. Precursors of MR I are too short-lived to be seen and kinetic details of the MR I formation cannot be resolved by the recording system. Experiments with somewhat better temporal resolution revealed completion of the MR I formation within about 100 μs. Details of the MR I decay are considered in a separate section below.

The initial increase in absorbance depends on the ratio of absorbance coefficients

of rhodopsin and of MR I at the measuring wavelength. From the data of Hubbard, Brown & Kropf (1959) for the frog and from the known absorbance spectrum of rhodopsin, this ratio can be estimated to be 1·24 at 475 nm wavelength. As the decay of MR I is significantly slower than its formation, little MR I will decay during the rapid rising phase in the recordings. Accordingly, at least a 20% increase in absorbance (i.e. increase with respect to the absorbance of rhodopsin) could be expected. The increase amounts to 40%, however, rather than to 20%, if the pre-flash

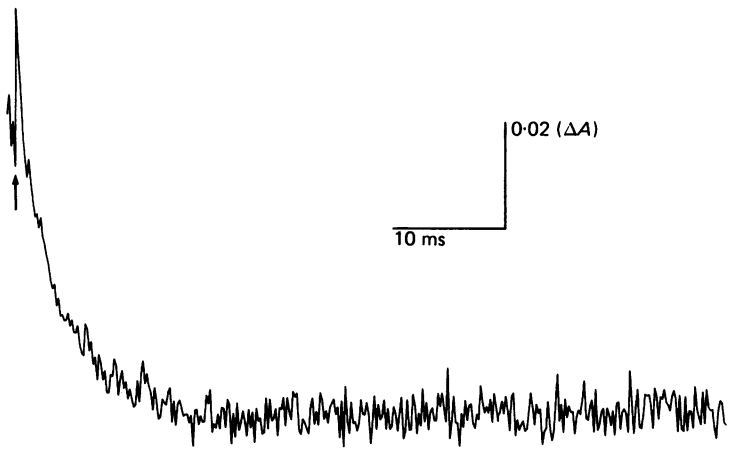

Fig. 1. Rapid absorbance change (ΔA) in a suspension of membrane vesicles from frog rod outer segments following the exposure to a strong yellow flash (arrow). Flash duration 120 μs; measuring wavelength 475 nm; pH 8·7.

level in Fig. 1 is compared with the level after 30 ms and if this absorbance loss is used as a reference for the initial rise. It should be noted that the final level of absorbance appearing stable on the millisecond scale of Fig. 1 is not stable on a minute scale. Fig. 2 shows that the absorbance changes occurring after the flash continue for another 200 min or longer. Before this time no stable level of absorbance is reached corresponding to zero concentration of all intermediates. The initial increase of absorbance amounts to about 20% with respect to this final level.

Slow changes of absorbance at 475 nm wavelength were measured according to the following schedule. Before the application of the bleaching flash a minimum period of 2 or 3 h was required until a slow drift of the signal became sufficiently small. In Fig. 2 this drift was 0·003 units of absorbance during the last hour before the flash. Values up to 0·005 were tolerated, and no corrections were made to compensate for this small error. The drift is presumably a consequence of the exposure of the preparations to red light during the dissection and setting-up procedures.

At the end of the pre-flash period the cuvette was momentarily positioned within the beam for the rapid reactions, and recordings as shown in Fig. 1 were made. The measurements of slow changes were continued about 10 s after the flash. This time was required for the low-pass filter to recover and is marked in the recordings by a big spike. Subsequently, the absorbance rises and approaches a maximum after about 5 min. The final part of the recording consists of a slow exponential decay. After about

200 min no further changes occur, and the final stable level of absorbance can be used to define the base line corresponding to zero concentration of the rhodopsin intermediates.

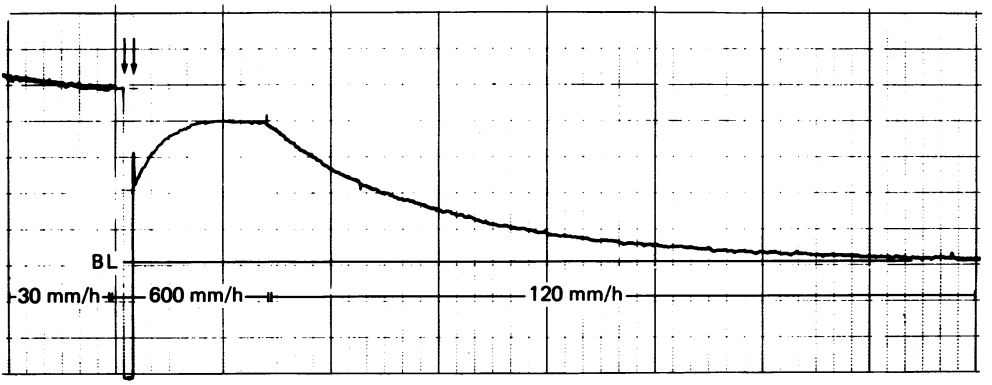

Fig. 2. Slow changes of absorbance in a suspension of membrane vesicles before and after exposure to a strong bleaching flash. The left arrow marks the end of the pre-flash period, the right arrow corresponds to the beginning of the post-flash period. Rapid changes (Fig. 1) were recorded during the interval between the arrows. Measuring wavelength 475 nm; recorder speeds as indicated; pH 8·7. Full scale of the ordinate corresponds to 0·2 units of absorbance. The stable level of absorbance reached after about 200 min defines the base line (BL). The spike at the begin of the pre-flash period is due to the slowly recovering low-pass filter. Same experiment as in Fig. 1.

Evaluation and pH dependence of the MR I concentration at equilibrium

Fig. 2 clearly shows that the slow reactions recorded after the flash start at a level which is different from zero. The data are normalized with respect to the pre-flash level as 1 and the final base line as zero. In the experiment shown, the starting point of slow changes is 0·42. It should be remembered that two intermediates of rhodopsin, i.e. MR I and MR III, appreciably absorb light of 475 nm wavelength. The formation of MR III is very slow, however, and, immediately after the flash, the concentration of MR III is negligible, so that the following equation holds (Baumann, 1978):

$$A_{475} = (\epsilon_{\mathrm{MR\ I}}/\epsilon_{\mathrm{R}})\,[\mathrm{MR\ I}]. \qquad (1)$$

A_{475} is the absorbance at 475 nm, normalized according to the total change at this wavelength; [MR I] is the relative concentration of this intermediate (i.e. concentration in proportion to the amount of rhodopsin bleached), and the ϵ values denote the respective absorbance coefficients of MR I and of rhodopsin (R) at 475 nm. The ratio of the two absorbance coefficients in eqn. (1) is known to be 1·24 (cf. p. 350). Therefore, at the starting point of slow reactions in Fig. 2, the relative concentration of MR I amounts to 0·42/1·24 = 0·34. This figure is the MR I concentration after virtual completion of the rapid reactions (cf. Fig. 1) and it represents an equilibrium in which MR I is one of the reactants.

The kinetics of both rapid and slow reactions are strongly influenced by the pH of the medium. The concentration of MR I at the end of the rapid changes decreases with decreasing pH. This is the expected behaviour as from earlier findings it is known

that the equilibrium between MR I and MR II is pH dependent and that low pH favours the formation of MR II (Matthews *et al.* 1963). Fig. 3 illustrates the non-linear relationship between MR I at the rapid equilibrium and pH. The data are fitted by a curve calculated from

$$[\text{MR I}]_{eq} = \frac{1}{a + b[H^+]}, \tag{2}$$

where the constants a and b are 2·2 and $4{\cdot}5 \times 10^8$, respectively. Fig. 3 resembles a titration plot but, unlike the conventional dissociation curve, which eventually approaches 1, the present curve levels off at about 0·45. It will be shown below that a and b are not merely empirical constants but can be defined within the framework of a kinetic model.

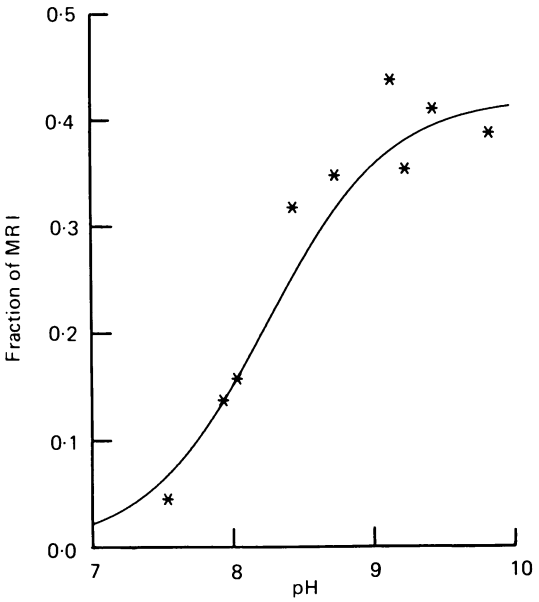

Fig. 3. Relative concentration of metarhodopsin I (MR I) calculated from eqn. (1) and plotted *vs.* pH of the medium (symbols). The curve represents eqn. (2) with constants $a = 2{\cdot}2$ and $b = 4{\cdot}5 \times 10^8$.

Kinetic analysis of the rapid reactions

A model for the rapid reactions must first of all explain the behaviour of MR I at equilibrium as described in Fig. 3. In addition, it must be compatible with the observed kinetics of the MR I–MR II transition. This reaction was previously treated as a reversible first-order process (Baumann, 1976, 1978). The experiments at different pH, however, revealed a more complex picture and led us to the following model:

$$\text{MR I} \underset{k_{21}}{\overset{k_{12}}{\rightleftharpoons}} \text{MR II}' \underset{k_{32}}{\overset{k_{23}}{\rightleftharpoons}} \text{MR II}''.$$

The scheme consists of two consecutive reactions, the reactants being one metarhodopsin I (MR I) and two isochromic forms of metarhodopsin II, here named MR II′

and MR II″. These two intermediates are assumed to have identical, or very similar, absorbance spectra, and their presence is inferred from their different kinetics. The existence of isochromic metarhodopsins was repeatedly postulated in the literature (cf. Knowles & Dartnall, 1977), and Emrich & Reich (1974) put forward a model with an equilibrium reaction between two isochromic forms of metarhodopsin II. The *k*s in the scheme are, at this stage of the analysis, treated as first-order rate constants. This may appear inadequate if the proton uptake during the MR I–MR II transition is remembered (Falk & Fatt, 1966). However, this simplification led to the final solution of the present analysis and must be described in some detail.

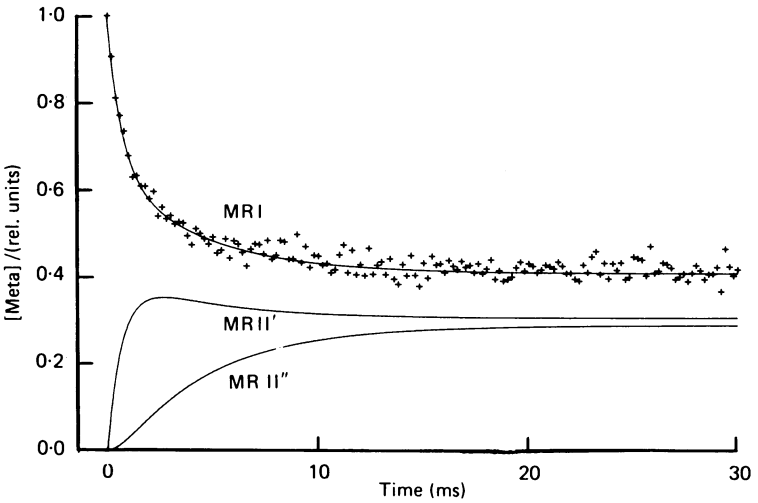

Fig. 4. Kinetics of rapid absorbance changes. Data points are from an experiment carried out at pH 9·4. The curves represent eqn. (A 1) (for MR I), eqn. (A 2) (for MR II′) and eqn. (A 3) (for MR II″), respectively, with the parameters $k_{12} = 558\ s^{-1}$, $k_{21} = 746\ s^{-1}$, $k_{23} = 170\ s^{-1}$ and $k_{32} = 180\ s^{-1}$.

Kinetic equations derived from the model may be found in the Appendix. Loss of MR I during its rapid formation from precursors was ignored, and the reactions were assumed to start at the MR I stage (i.e. MR I = 1 at the time $t = 0$). Accordingly, the data were normalized with respect to the sharp peak occurring a few hundred microseconds after the flash (Fig. 1). The normalization took into account that MR I approached an equilibrium concentration after some 20 or 30 ms and that this concentration is given by the data shown in Fig. 3. Numerical values for the rate constants were determined with the aid of a computer program designed for non-linear regression analysis and based on Marquardt's algorithm (Marquardt, 1963; Robinson, 1977). Sets of fifty-five or seventy-three data pairs together with eqn. (A 1) were used to estimate the k values by minimizing the sum-of-squares function. All computations converged after some twenty-five iterations. The quality of fit that can be achieved may be assessed from the upper curve and the data points in Fig. 4. Confidence limits for the parameters (rate constants) of the experiment shown were as follows: k_{12}, $\pm 12\,\%$; k_{21}, $\pm 27\,\%$; k_{23}, $\pm 50\,\%$; k_{32}, $\pm 23\,\%$ (for details see Robinson, 1977).

Fig. 4 shows details of the double equilibrium at pH 9·4. Two exponentials are

required for an adequate description of the MR I behaviour (upper curve). The first and more rapid decay has a mirror image in the formation of MR II′ which, in its rising part, is equally rapid and then runs through a maximum (middle curve). The formation of MR II″ is somewhat slower and is described by a sigmoid-shaped function (lower curve). It should be noted that, at 380 nm, the rise of absorbance due to the formation of the metarhodopsins II would be proportional to the sum of the two lower curves which would form the mirror image of the upper curve.

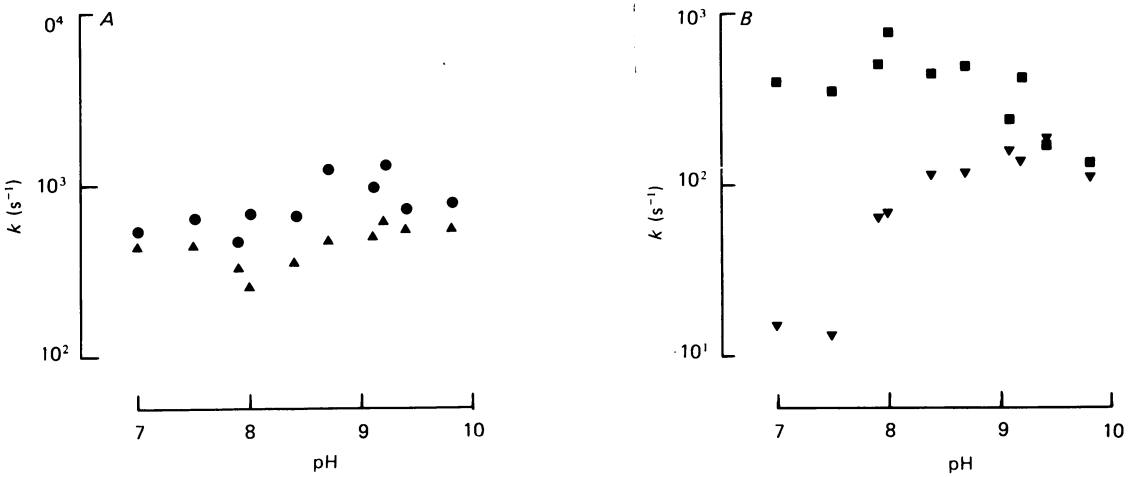

Fig. 5. Rate constants of the rapid reactions plotted against pH. *A*, k_{12} (▲) and k_{21} (●); *B*, k_{23} (■) and k_{32} (▼).

Although the model can adequately account for the observed kinetics, it is incomplete so long as it cannot explain the effect of pH on the reactions. In Fig. 5, the various rate constants are plotted against pH. It is obvious that pH has little influence on the constants k_{12} and k_{21}. This finding suggests that so far as the MR I to MR II′ transition is concerned, the model is correct, i.e. the first step may be treated as a reversible first-order reaction.

The situation is different with respect to the second equilibrium. Here, the constant k_{23} likewise shows little change with increasing pH. Two values of k_{23}, i.e. at pH 9·4 and 9·8, are smaller than the average, but within most of the range k_{23} remains remarkably constant. The fourth constant of the model, however, seems to depend systematically on pH. From pH 7 to pH 9·8, k_{32} increases by a factor 10 or so, and one might speculate whether a hydroxyl ion catalysis is involved when MR II″ reverts to MR II′ (Emrich & Reich, 1974). On the other hand, the MR I–MR II transition has long been known to be accompanied by a proton uptake (Falk & Fatt, 1966; McConnell, Rafferty & Dilley, 1968; Ostroy, 1974). Therefore, modifications of the model which can account for this observation should be considered.

The pH-dependent equilibrium of the MR I–MR II transition

If one of the metarhodopsins (MR) behaves like a base and can take up a proton according to

$$MR + H^+ \rightleftharpoons MRH^+$$

then an equilibrium constant

$$K = \frac{[MRH^+]_{eq}}{[MR]_{eq}[H^+]} \tag{3}$$

can be defined, where the subscript 'eq' indicates equilibrium concentrations of the base (MR) and of the conjugate acid (MRH^+). The equilibrium concentrations of the

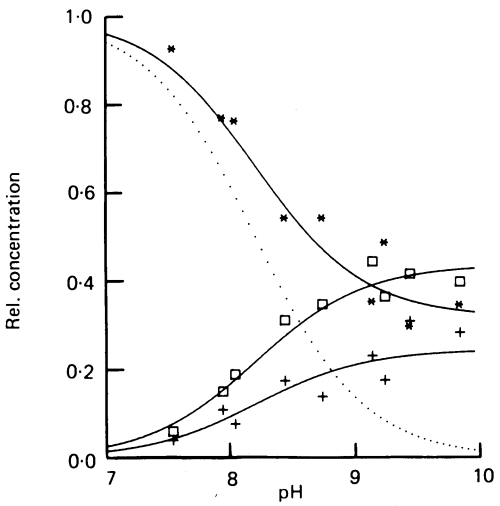

Fig. 6. Influence of pH on the equilibria of the rapid reactions. Equilibrium concentrations of MR I (□), MR II′ (+) and MR II″ (*) are calculated from eqns. (A 1), (A 2) and (A 3) with the parameters of Fig. 5. The curves represent eqn. (8) (lower continuous curve), eqn. (9) (middle continuous curve), eqn. (10) plus eqn. (11) (upper continuous curve), and eqn. (11) (dotted curve).

three metarhodopsins considered in the preceding section are known and are plotted as functions of pH in Fig. 6. Within the range covered, the ratio between $[MR\ I]_{eq}$ and $[MR\ II']_{eq}$ remains fairly constant, hence protons are not directly involved in this reaction. Accordingly, the equilibrium constant may be defined as

$$K_1 = \frac{[MR\ II']_{eq}}{[MR\ I]_{eq}} = 0{\cdot}56. \tag{4}$$

The numerical figure is an estimate from the data in Fig. 5 (k_{12}/k_{21}).

One might now expect that MR II′ and MR II″ would behave like an acid–base pair (Emrich & Reich, 1974). But they do not because if MR II″ were an acid of the form $MR\ II''H^+$ it should release its proton at alkaline pH and, with increasing pH, its concentration should approach zero. As this is not the case (see the asterisks in

Fig. 6), MR II″ is probably not a homogeneous compound but represents that presumed acid–base pair, i.e.

$$\text{MR II}'' + \text{H}^+ \rightleftharpoons \text{MR II}''\text{H}^+.$$

The establisment of this equilibrium is likely to be extremely rapid (Bell, 1959) and would not be resolved by the recording system. It seems justified, therefore, to extend the scheme of rapid reactions in the following way:

$$\text{MR I} \underset{k_{21}}{\overset{k_{12}}{\rightleftharpoons}} \text{MR II}' \underset{k_{32}}{\overset{k_{23}}{\rightleftharpoons}} \text{MR II}'' + \text{H}^+ \rightleftharpoons \text{MR II}''\text{H}^+,$$

where the rate constants of the reversible proton uptake are unknown. In addition to the equilibrium constant K_1, one can define

$$K_2 = \frac{[\text{MR II}'']_{eq}}{[\text{MR II}']_{eq}} \tag{5}$$

and

$$K_3 = \frac{[\text{MR II}''\text{H}^+]}{[\text{MR II}'']_{eq}[\text{H}^+]} \tag{6}$$

for the second and third equilibria of the scheme. For the sum of concentrations, one may write

$$[\text{MR I}] + [\text{MR II}'] + [\text{MR II}''] + [\text{MR II}''\text{H}^+] = 1. \tag{7}$$

From eqns. (4), (5), (6) and (7) functions may be derived that illustrate the dependence on pH of the various equilibrium concentrations:

$$[\text{MR I}]_{eq} = 1/a \tag{8}$$

$$[\text{MR II}']_{eq} = K_1/a \tag{9}$$

$$[\text{MR II}'']_{eq} = K_1K_2/a \tag{10}$$

$$[\text{MR II}''\text{H}^+]_{eq} = K_1K_2K_3[\text{H}^+]/a \tag{11}$$

with $$a = 1 + K_1 + K_1K_2 + K_1K_2K_3[\text{H}^+].$$

In Fig. 6, these functions are used to fit the data points. The following figures were found to give an optimum fit (assessed by eye): $K_1 = 0{\cdot}56$, $K_2 = 1{\cdot}3$ and $K_3 = 5 \times 10^8$ mol^{-1} l. The extended scheme thus confirms that there are two metarhodopsins II but that only one of them can rapidly take up or release a proton. The observed dependence on pH of the equilibrium concentration of MR I (Fig. 3) is indirect and is a consequence of the rapid equilibrium between the base MR II″ and its conjugate acid.

The reciprocal of the equilibrium constant K_3 corresponds to a pK of about 8·7. One must not expect, however, that this figure is represented by the turning point of the function $[\text{MR II}''\text{H}^+] = f(\text{pH})$. The dotted curve in Fig. 6 suggests a pK at a more acid pH but this is erroneous and is due to the interaction of the proton-dependent step with the other reversible reactions.

The four-parameter scheme used for the kinetic analysis is correct as long as the concentration of MR II″H$^+$ is small and the simplification $[\text{MR II}''] \approx$

([MR II″]+[MR II″H$^+$]) holds. At low pH, however, a substantial fraction of MR II″H$^+$ will be formed at the expense of MR II″, and a systematic error will influence the kinetic analysis. This is most obvious in the rate equation for MR II″

$$\frac{\mathrm{d}[\text{MR II}'']}{\mathrm{d}t} = -k_{32}[\text{MR II}'']+k_{23}[\text{MR II}']. \tag{12}$$

Here, the term k_{32}[MR II″] is not only a function of time but also a function of pH. According to the regression analysis, the rate constant k_{32} seems to be the pH-dependent factor (cf. Fig. 5). This is an artifact, however, and is the consequence of the above-mentioned simplification, which is no longer justified at low pH where ([MR II″]+[MR II″H$^+$]) is considerably larger than [MR II″] alone. At pH 7·5, k_{32} is presumably as large as it is at pH 9·4 but as the sum ([MR II″]+[MR II″H$^+$]) is about 30 times larger than [MR II″] alone (Fig. 6), k_{32} appears to be one decade smaller than it really is.

Quantitative analysis of slow reactions

The slow decay reactions during the bleaching of rhodopsin start at the MR II stage. MR II is hydrolysed to retinal and opsin (Matthews *et al.* 1963), and a fraction of it may decay through MR III. Reversal from MR III to MR II was discussed within the framework of kinetic models (Baumann, 1972; Baumann & Reinheimer, 1973; Ernst, Kemp & White, 1978) but until recently there was no direct evidence for this reaction. Chabre & Breton (1979) have measured the linear dichroism of slowly decaying rhodopsin intermediates and, from their results, an equilibrium between MR II and MR III may be inferred. Alterations of pH can influence this equilibrium, and a kinetic model must account for this effect.

A reaction of the type

$$\text{MR III}+\text{H}^+ \rightleftharpoons \text{MR IIH}^+$$

is unlikely because this would be a rapid process whereas the reactions between MR II and MR III following sudden changes of pH are slow and quite unlike a quickly established acid–base equilibrium (Chabre & Breton, 1979). Accordingly, the MR II″H$^+$ compound can be ruled out as a direct partner in a reversible reaction with MR III.

For the further analysis the following model will be employed:

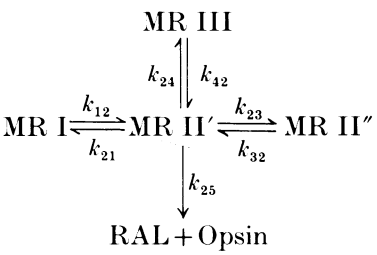

where RAL denotes all-*trans*-retinal. The scheme ignores the fact that MR II″ can take up protons (this is a simplification the sequels of which are considered below).

An alternative scheme with an equilibrium between MR II″ and MR III was also considered and gave similar results with respect to that equilibrium (so long as the analysis was confined to experiments at high pH).

The above model requires that seven rate constants be found. Fortunately, the constants k_{24}, k_{42} and k_{25} are all likely to be several orders of magnitude smaller than the constants for the rapid reactions which therefore will not measurably be influenced by the slow ones. The slow reactions, on the other hand, start at concentration levels set by the rapid double equilibrium. The extremely different magnitudes of the rate constants in the model lead to a system of stiff differential equations. A possible way of estimating the rate constants would be to work out a computer routine in which the integration of stiff equations is combined with a

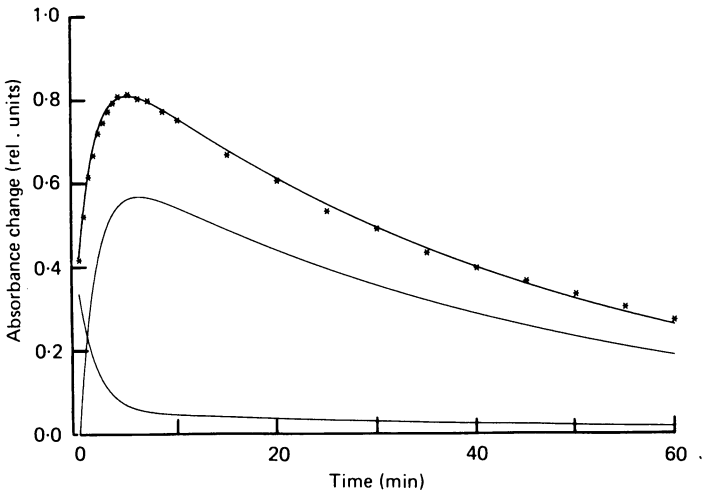

Fig. 7. Slow absorbance change at 475 nm wavelength. Data (*) are from the experiment of Fig. 2. The upper curve represents eqn. (13). The two lower curves are relative concentrations of MR III (with maximum) and MR I (decaying) derived from the above model; the parameters are found in Figs. 5, 8 and 9.

least-squares procedure, i.e. the result of the numerical integration should be compared with the experimental data and, by choosing suitable values of the various ks, a sum-of-squares function should be minimized. To carry out the first step, an integration routine for stiff equations (Gear's method; cf. Hall & Watt, 1976, chapter 13) was used with values of k_{12}, k_{21}, k_{23} and k_{32} from the rapid reactions and with preliminary estimates for k_{24}, k_{42} and k_{25}. The latter constants were then varied in a trial-and-error manner until the error mean square was smaller than a previously set value (5×10^{-4}). The quality of fit that could be achieved by this method may be assessed from Fig. 7.

The data for the quantitative analysis of slow reactions were taken from experiments like the one shown in Fig. 2. Normalization was carried out again with respect to the pre-flash level as 1 and the final base line as zero, and the function

$$A_{475} = (\epsilon_{\mathrm{MR\ I}}/\epsilon_{\mathrm{R}})[\mathrm{MR\ I}] + (\epsilon_{\mathrm{MR\ III}}/\epsilon_{\mathrm{R}})[\mathrm{MR\ III}] \qquad (13)$$

was used to fit the data (Baumann, 1978). The ratio $\epsilon_{\mathrm{MR\ I}}/\epsilon_{\mathrm{R}}$ is the same as in eqn.

(1), and $\epsilon_{MR\ III}/\epsilon_R = 1{\cdot}29$ may be derived from the results of Chabre & Breton (1979) and from the known absorbance spectrum of rhodopsin. In Fig. 7 the two lower curves represent [MR I](t) and [MR III](t), respectively: MR III starts at zero concentration and reaches a maximum after about 6 min while MR I decays in two phases at obviously different rates. These curves can be thought of as results of the numerical integration but their actual mathematical form is simple. They are combinations of two exponentials, and their exponents and coefficients may be taken from the results of integration.

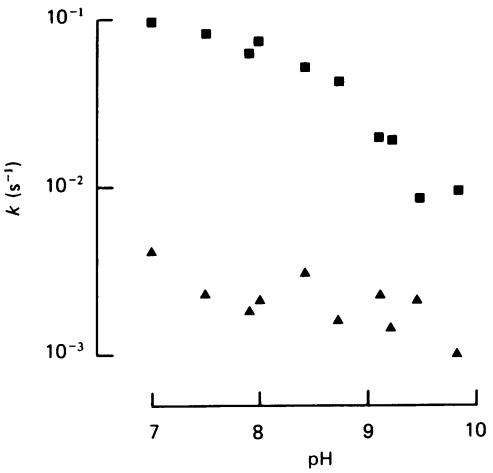

Fig. 8. Rate constants k_{24} (squares) and k_{42} (triangles) of the equilibrium reaction between metarhodopsin II′ and metarhodopsin III plotted *vs.* pH.

The reaction scheme was used to analyse ten experiments carried out in the range of pH 7 to 9·8. On the more acid side of this range the presence of the protonated compound MR II″H^+ cannot be ignored and, there, the scheme is no longer correct. If it is nevertheless used, an apparent dependence on pH of one of the rate constants results. The effect is seen in Fig. 8 where the rate constant k_{24} controlling the formation of MR III is growing with decreasing pH. This growth, however, is not genuine but is a consequence of the protonation of MR II″. If a substantial fraction of MR II″ exists as MR II″H^+, then the concentrations of both MR II′ and or MR II″ are low (Fig. 6). As the rate of formation of MR III is mainly dependent on the product k_{24}[MR II′], the abnormally high value of k_{24} compensates for the small figure of [MR II′]. It must be added, however, that this artifact is of little significance if the medium is alkaline. For pH > 9, similar results are obtained with all models in which an equilibrium between MR III and one of the MR II compounds is considered. The rate constant for the formation of MR III (k_{24} or k_{34}) is on the average $1{\cdot}6 \times 10^{-2}$ s^{-1}, the rate constant for the reversal of this reaction (k_{42} or k_{43}) is $1{\cdot}8 \times 10^{-3}$ s^{-1}, and the equilibrium constant

$$K_4 = \frac{[\text{MR III}]_{eq}}{[\text{MR II}']_{eq}} = \frac{k_{24}}{k_{42}} \tag{14}$$

is at least 9. This fairly high value accounts for the observations of Bowmaker (1973) and of Chabre & Breton (1979) that even at pH 5 a measurable fraction of MR III

may be seen. The dependence on pH of $[\text{MR III}]_{eq}$ may be computed with the aid of

$$[\text{MR III}]_{eq} = \frac{K_1 K_4}{1 + K_1 + K_1 K_2 + K_2 K_4 + K_1 K_2 K_3 [H^+]}, \quad (15)$$

which obtains if all metarhodopsins are in equilibrium with each other.

The decay reactions of the metarhodopsins end with the hydrolysis to retinal and opsin. In the scheme, this hydrolysis is associated with the MR II′ compound (though hydrolysis of MR II″ is also conceivable). The hypothesis that MR III is split by

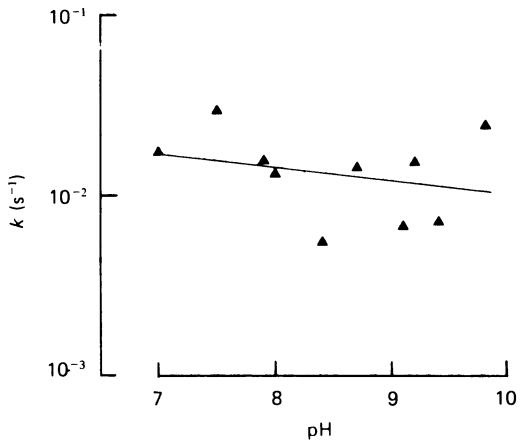

Fig. 9. Rate constant (k_{25}) of the hydrolysis of metarhodopsin II′ *vs.* pH. The regression line suggests a slight increase with decreasing pH.

hydrolysis (in an equilibrium model) was considered and rejected in an earlier study (Baumann, 1972). In Fig. 9, the rate constant of the hydrolysis (k_{25}) is plotted as a function of pH. An effect of pH upon this constant is not very obvious and the data scatter around a mean value of $1{\cdot}3 \times 10^{-2}$ s^{-1}. However, the regression line suggests a slight tendency of increase with decreasing pH. This would be in line with a general rule for the hydrolysis of Schiff base linkages, viz., the reaction is acid-catalysed.

DISCUSSION

The kinetic schemes in the present analysis are appropriate to a homogeneous system. A suspension of membrane vesicles, however, consists of two compartments, the spaces inside and outside the vesicles. This is of relevance if protons from the surroundings bind to one of the metarhodopsins in the membrane. It is conceivable that a major fraction of reactive sites faces the inner surface of the vesicles and that the number of protons available from the interior of the vesicles is too small to allow for the complete protonation of MR II″. If, in addition, the vesicle membrane were weakly permeable (or impermeable) to protons, then a complicated two-compartment analysis would be required. The real situation, however, seems to be less unfavourable. The membrane vesicles for the present study were prepared from rod outer segments by sonication. The membrane sidedness in these vesicles may be assumed to be almost

homogeneous and the same as in intact disks (Adams, Tanaka & Shichi, 1978; Nakano, Ikai, Nishigai & Noda, 1979; see also Hubbell, Fung, Hong & Chen, 1977). As regards the groups involved in the proton uptake, one would preferably consider groups with an appropriate pK and with an intramolecular location favourable for an exchange of protons with the surroundings. Sulphhydryl groups meet both conditions. their pK (8–9) corresponds to the one found in this study (8·7) and they are situated in a part of the rhodopsin molecule that projects out of the cytoplasmic surface of the disk membrane (Hubbell & Bownds, 1979). If the formation of MR II″ is associated with the exposure of a sulphydryl group to the cytoplasm (buffer), a free and rapid exchange of protons could occur.

The reactions of the metarhodopsins have been analysed over a pH range from 7 to 9·8. No spectroscopic changes could be measured at pH > 10. Although this observation was not systematically investigated, it may be assumed that frog rhodopsin is not stable at pH $\geqslant$ 10 (cf. Radding & Wals, 1956). At acid pH values (< 7) a relatively stable intermediate interferes with the quantitative analysis. This intermediate is presumably *N*-retinylidene-opsin$_{440}$ (NRO_{440}). It is formed more slowly than MR III and its absorbance at 475 nm is superimposed upon that of MR III. Owing to the very slow decay of NRO_{440} a final stable level of absorbance was not reached within a reasonable time span, and the experiments at pH 5 and 6 were terminated before a zero line as described in the first part of the Results section could be defined. Therefore, the equilibrium concentration of MR I was unknown, and this rendered the quantitative analysis unachievable. Even in the absence of NRO_{440} the quantitative analysis would have been difficult. The equilibrium concentrations of MR I at the more acid pH become very small and cannot be determined with sufficient accuracy. The intracellular pH of intact frog rods is unknown. It may be close to pH 7 although frog blood (and presumably the extracellular medium around the rods) is fairly alkaline, i.e. 7·9 at 15 °C (Rahn, 1966). If protons are distributed according to the Donnan equilibrium, then a presumed membrane potential of −40 mV gives rise to a pH difference of 0·7 units and the intracellular pH would be 7·2. For frog metarhodopsin, pH 7·2 is on the more acid side of the titration curve (Fig. 6) where most of MR II is encountered as a protonated compound.

According to the present results, there are four metarhodopsins which can all react with one another within the framework of coupled reversible reactions. One of the metarhodopsins II exists in two forms, (i) as the deprotonated MR II″ and (ii) as the protonated MR II″H^+. The rapid equilibrium between these two compounds provides the common basis of all pH effects observed in this study. The reaction scheme is complex but, in a way, it is merely an assemblage of earlier findings. In previous kinetic studies, simultaneous first-order reactions were used to describe the conversion of MR I to MR II, and two (frog rhodopsin) or three (bovine rhodopsin) rate constants were extracted from the data (Wulff, Adams, Linschitz & Abrahamson, 1958; Falk & Fatt, 1966). On the other hand, Matthews *et al.* (1963) worked out the details of an equilibrium between MR I and MR II. If the two types of results are to be reconciled with one another, a kinetic model involving a double (or triple) equilibrium is adequate. It can predict the MR I decay as a sum of exponentials (eqn. A 1), and equilibrium concentrations can be taken into account. In an earlier kinetic study of

slow reactions (Baumann, 1972) a model with parallel pathways of MR II decay was preferred over an equilibrium model which, though confined to the slow reactions, was a predecessor of the present scheme. The data of Chabre & Breton (1979) now clearly support the equilibrium model, and the pH effects associated with the MR II–MR III reaction (see also Bowmaker, 1973) neatly fit the results of the present analysis.

The MR I–MR II transition is usually considered to involve sizeable conformational rearrangements of opsin (Kropf, 1972). According to the present analysis, the transition proceeds in two steps. The first one, MR I to MR II′, is accompanied by a large hypsochromic shift ($\Delta\lambda_{max} \approx 100$ nm) but is not influenced by the external pH (Fig. 5). This means that although the interaction between the chromophore and the opsin changes rather dramatically, this change is an intramolecular event and is not dependent on the pH of the environment. The second step, MR II′ to MR II″, is isochromic and implies the exposure of a titratable group. Therefore, MR II″ is encountered either as a protonated (MR II″H^+) or as a deprotonated (MR II″) compound. The acid–base reaction seems to occur in a more peripheral part of the molecule where protons can freely be exchanged with the surroundings. From there, the influence upon the chromophore is apparently too weak to induce a noticeable spectral shift. On the whole, the MR I to MR II transition may be interpreted as a two-step unfolding of the opsin in which the first change involves the closer environment of the chromophore whereas the second step merely occurs in the periphery of the molecule and at a greater distance from the chromophoric site. The slow formation of MR III could be a partial refolding from the MR II′ stage to a rather stable conformation which, so far as the absorbance spectrum is concerned, resembles MR I. Donner & Hemilä (1975) observed that little or no MR III is detected if the fraction of rhodopsin bleached is substantially smaller than in the present study. The reaction scheme used here does not provide an explanation for the absence of MR III following very small bleaches. However, the problem is confined to one step, i.e. the hydrolysis of MR II′. If this reaction is assumed to become more rapid at lower concentration levels, then less MR III would be accumulated. One might postulate that an enzyme is involved in the hydrolysis of MR II′. The enzyme would be efficient at low bleaching levels but would be saturated or inhibited (or both) after substantial bleaches. There is no evidence for the existence of such an enzyme but the question should be considered in future investigations.

APPENDIX

Kinetic equations for the rapid reactions. With the initial conditions MR I = 1, MR II′ = MR II″ = 0 at $t = 0$, the equations read

$$\text{MR I} = k_{21}k_{32}/s_1 s_2 - m_1 \exp(-s_1 t) - m_2 \exp(-s_2 t) \quad \text{(A 1)}$$

$$\text{MR II}' = k_{12}k_{32}/s_1 s_2 - n_1 \exp(-s_1 t) - n_2 \exp(-s_2 t) \quad \text{(A 2)}$$

$$\text{MR II}'' = 1 - (\text{MR I} + \text{MR II}'), \quad \text{(A 3)}$$

where $s_1 = -x_1$, $s_2 = -x_2$ and $x_{1,2}$ are the roots of the equation

$$x^2 + x(k_{12} + k_{21} + k_{23} + k_{32}) + (k_{12}k_{23} + k_{21}k_{23} + k_{21}k_{32}) = 0.$$

In addition,

$$m_1 = \frac{s_1^2 - s_1(k_{21} + k_{23} + k_{32}) + k_{21}\,k_{32}}{s_1(s_2 - s_1)},$$

$$m_2 = \frac{s_2^2 - s_2(k_{21} + k_{23} + k_{32}) + k_{21}\,k_{32}}{s_2(s_1 - s_2)},$$

$$n_1 = \frac{k_{12}(k_{32} - s_1)}{s_1(s_2 - s_1)},$$

$$n_2 = \frac{k_{12}(k_{32} - s_2)}{s_2(s_1 - s_2)}.$$

This investigation was supported by the Deutsche Forschungsgemeinschaft. Part of this work was presented by W. Zeppenfeld to the Medical Faculty of the Justus Liebig-University Giessen in partial fulfilment of the requirements for the degree of Doctor of Dentistry. We thank Dr W. Seidel for helpful discussions and Dr A. Ostermann for computing assistance.

REFERENCES

ADAMS, A. J., TANAKA, M. & SHICHI, H. (1978). Concanavalin A binding to rod outer segment membranes: usefulness for preparation of intact disks. *Expl Eye Res.* **27**, 595–605.

BAUMANN, CH. (1972). Kinetics of slow thermal reactions during the bleaching of rhodopsin in the perfused frog retina. *J. Physiol.* **222**, 643–663.

BAUMANN, CH. (1976). The formation of metarhodopsin$_{380}$ in the retinal rods of the frog. *J. Physiol.* **259**, 357–366.

BAUMANN, CH. (1978). The equilibrium between metarhodopsin I and metarhodopsin II in the isolated frog retina. *J. Physiol.* **279**, 71–80.

BAUMANN, CH. & REINHEIMER, R. (1973). Temperature dependence of slow thermal reactions during the bleaching of rhodopsin in the frog retina. In *Biochemistry and Physiology of Visual Pigments*, ed. LANGER, H., pp. 89–99. Berlin: Springer.

BELL, R. B. (1959). *The Proton in Chemistry*. Ithaca: Cornell University Press.

BOWMAKER, J. K. (1973). The photoproducts of retinal-based visual pigments *in situ*: a contrast between *Rana pipiens* and *Gekko gekko*. *Vision Res.* **13**, 1227–1240.

CHABRE, M. & BRETON, J. (1979). The orientation of the chromophore of vertebrate rhodopsin in the 'meta' intermediate states and the reversibility of the meta II–meta III transition. *Vision Res.* **19**, 1005–1018.

DONNER, K. O. & HEMILÄ, S. (1975). Kinetics of long-lived rhodopsin photoproducts in the frog retina as a function of the amount bleached. *Vision Res.* **15**, 985–995.

EMRICH, H. M. & REICH, R. (1974). Über Primärreaktionen beim Sehvorgang. Thermodynamischer und kinetischer Einfluss des pH-Wertes auf die Metarhodopsin-I–II-Umwandlung. Protonenverbrauch als Auswirkung einer Konformationsänderung. *Z. Naturf.* **29c**, 577–591.

ERNST, W., KEMP, C. M. & WHITE, H. A. (1978). Studies on the effect of bleaching amphibian rods *in situ*. II. The kinetics of slow bleaching reactions in the axolotl retina. *Expl Eye Res.* **26**, 337–350.

FALK, G. & FATT, P. (1966). Rapid hydrogen ion uptake of rod outer segments and rhodopsin solutions on illumination. *J. Physiol.* **183**, 211–224.

HAGINS, W. A. & YOSHIKAMI, S. (1975). Ionic mechanism in excitation of photoreceptors. *Ann. N.Y. Acad. Sci.* **264**, 314–325.

HALL, G. & WATT, J. M. (1976). *Modern Numerical Methods for Ordinary Differential Equations*. Oxford: Clarendon Press.

HUBBARD, R., BROWN, P. K. & KROPF, A. (1959). Action of light on visual pigment. Vertebrate lumi- and metarhodopsins. *Nature, Lond.* **183**, 442–446.

HUBBELL, W. L. & BOWNDS, M. D. (1979). Visual transduction in vertebrate photoreceptors. *A. Rev. Neurosci.* **2**, 17–34.

HUBBELL, W. L., FUNG, K.-K., HONG, K. & CHEN, Y. S. (1977). Molecular anatomy and light-dependent processes in photoreceptor membranes. In *Vertebrate Photoreception*, ed. BARLOW, H. B. & FATT, P., pp. 41–59. New York & London: Academic Press.

KNOWLES, A. & DARTNALL, H. J. A. (1977). *The Eye*, vol. 2B, *The Photobiology of Vision*, ed. DAVSON, H. New York & London: Academic Press.

KROPF, A. (1972). The structure and reaction of visual pigments. In *Handbook of Sensory Physiology*, vol. VII/2, ed. FUORTES, M. G. F., pp. 239–278. Berlin: Springer.

MCCONNELL, D. G., RAFFERTY, C. N. & DILLEY, R. A. (1968). The light-induced proton uptake in bovine retinal outer segment fragments. *J. biol. Chem.* **243**, 5820–5826.

MARQUARDT, D. W. (1963). An algorithm for least-squares estimation of nonlinear parameters. *J. Soc. indust. appl. Math.* **11**, 431–441.

MATTHEWS, R. G., HUBBARD, R., BROWN, P. K. & WALD, G. (1963). Tautomeric forms of metarhodopsin. *J. gen. Physiol.* **47**, 215–240.

NAKANO, T., IKAI, A., NISHIGAI, M. & NODA, H. (1979). Orientation of the rhodopsin sugar moiety in bovine disk membrane. *J. Biochem.* **85**, 1339–1346.

OSTROY, S. E. (1974). Hydrogen ion changes of rhodopsin. *pK* changes and the thermal decay of metarhodopsin II_{380}. *Arch. Biochem. Biophys.* **164**, 275–284.

RADDING, C. M. & WALD, G. (1956). The stability of rhodopsin and opsin. Effects of pH and aging. *J. gen. Physiol.* **39**, 923–933.

RAHN, H. (1966). Evolution of the gas transport system in vertebrates. *Proc. R. Soc. Med.* **59**, 493–494.

REUTER, T. (1976). Photoregeneration of rhodopsin and isorhodopsin from metarhodopsin III in the frog retina. *Vision Res.* **16**, 909–917.

ROBINSON, B. (1977). *SPSS subprogram NONLINEAR: nonlinear regression*. Manual No. 433. Evanston, Ill.: Vogelback Computing Center, Northwestern University.

SAITO, Z. (1938). Isolierung der Stäbchenaussenglieder und spektrale Untersuchung des daraus hergestellten Sehpurpurextraktes. *Tohoku J. exp. Med.* **32**, 432–446.

WALKER, J. L. & BROWN, H. M. (1977). Intracellular ion activity measurements in nerve and muscle. *Physiol. Rev.* **57**, 729–778.

WULFF, V. J., ADAMS, R. G., LINSCHITZ, H. & ABRAHAMSON, E. W. (1958). Effects of flash illumination on rhodopsin in solution. *Ann. N.Y. Acad. Sci.* **74**, 281–290.